Title	Comparison of MADYMO and physical models for brain injury reconstruction
Authors(s)	Post, Andrew, Hoshizaki, Thomas Blaine, Gilchrist, M. D.
Publication date	2014-05-04
Publication information	Post, Andrew, Thomas Blaine Hoshizaki, and M. D. Gilchrist. "Comparison of MADYMO and Physical Models for Brain Injury Reconstruction" 19, no. 3 (May 4, 2014).
Publisher	Informa UK (Taylor & Francis)
Item record/more information	http://hdl.handle.net/10197/5934
Publisher's statement	This is an electronic version of an article published in International Journal of Crashworthiness (2014) 19(3): 301-310. International Journal of Crashworthiness is available online at: www.tandfonline.com, DOI: http://dx.doi.org/10.1080/13588265.2014.897413.
Publisher's version (DOI)	10.1080/13588265.2014.897413

Comparison of MADYMO and physical models for brain injury reconstruction

Andrew Post[a], T. Blaine Hoshizaki[a], Michael D. Gilchrist[b,a]

Human Kinetics, University of Ottawa, Ottawa, Canadaa

School of Mechanical & Materials Engineering, University College Dublin, Dublin, Irelandb

Corresponding author: Andrew Post (apost@uottawa.ca) 200 Lees Ave., room A106, Ottawa, Ontario, Canada, K1N 6N5 – phone number: +1 (613)5625800 ext 7210

Comparison of MADYMO and physical models for brain injury reconstruction

Brain injury is researched using physical, mathematical, anatomical, and computational models. However there has been little research to quantify the expected differences between these methods of brain injury research. The purpose of this research was to compare the brain deformation responses of identical traumatic brain injury (TBI) reconstructions, which were conducted first with Mathematical Dynamic Models (MADYMO) and then again with a Hybrid III headform. The ensuing finite element modeling was done using the University College Dublin Brain Trauma Model. The brain deformation parameters were analyzed in discrete regions of interest which matched the TBI lesion as identified on computed tomography scans of the subject. The results indicated that overall the Hybrid III provided responses which were of considerably larger magnitude than the MADYMO simulation for all metrics analyzed. The larger magnitude responses are likely a product of the more rigid nature of the Hybrid III in comparison to the MADYMO simulations. Interestingly, when the results are compared to the literature, the Hybrid III results match well with mTBI and TBI research, while the MADYMO simulations produce what would be considered very low local brain deformation responses for TBI lesions.

Keywords: Traumatic brain injury, Injury Reconstruction, MADYMO, Concussion

Introduction

Brain injury is a topic which has seen an increase in research in recent years. This research has been conducted following two streams, traumatic brain injury research and concussion research. Traumatic brain injury (TBI) is one of the leading causes of morbidity and mortality in Canada and the United States with more than 1.7 million cases every year [31]. Recently, concussion has also become a more prevalent issue in society due to the possible long term degenerative effects that these impacts can have on an individual[18,22,29]. The primary avenue of TBI and concussion research is to

reconstruct the event using a variety of models, typically physical, anatomical, and computational in an effort to find variables to understand their mechanisms [25].

The use of models to examine the mechanism of brain injury is common as it is ethically questionable to cause brain injuries on human subjects. Early work examining the mechanism of brain injury was conducted using cadavers and investigated the relationships between impact induced linear acceleration and pressure waves inside the cranium which were thought to be related to how the brain was damaged [32]. This research using physical cadaver models also gave insight into how the skull fractured, as well as how local deformation and the interior geometry of the skull could influence the occurrence of contusions and cerebral bleeds [7]. Further investigations into the influence of linear translation expanded into the realm of rotational acceleration with Gennerelli's [9] work using animal models. This extensive work using monkeys demonstrated that the application of rotational acceleration was able to create many types of brain injury, in the absence of linear acceleration. In addition to this work, Gurdjian and Lissner [8] induced concussive injuries to dogs to examine the relationship between intracranial pressure and acceleration magnitudes and durations. This research using animal and cadaver models demonstrated that TBI and concussive injuries have associations with linear and rotational acceleration [8,9,32].

There have been other models in use for brain injury research. Using basic physical models of the human brain, Holbourn [11] demonstrated how rotational acceleration can cause diffuse strains in the brain tissue; as these are considered to be a primary cause of subdural heomatoma (SDH) and concussion. More recently Bradshaw et al [3] used a physical model of the human skull and brain to demonstrate the mechanisms of subdural hematoma and diffuse axonal injury, indicating that impact kinematics, and rotational acceleration in particular has a significant influence on the

presence of these diffuse TBI injuries. This early work on brain injury using cadaver, animal, and basic physical models demonstrated that the continuum of brain injury can be traced back to impact induced motions [25]. However, the models used have some limitations when attempting to interpret their results in the context of the human system. The cadaver models are the closest representation of the human skull brain complex, however the results of the impacts are influenced by the preparation of the cadaver for the impact, in particular the perfusion of the vascular system and degradation of tissues. Animal models have the benefit of producing live responses from an impact, but as a result of differing material properties and brain size/geometries thresholds and mechanisms of injury for the brain may differ somewhat from the human. The basic physical models mentioned previously have a great benefit in that they can produce proof of concept for the mechanism of injury for the brain without requiring cadavers or injuring animals, but they lack the complexity of the human system and as a result their conclusions must be examined in that context.

More recently, with the improvement of technology, much brain injury research has focused on using physical and computational models to reconstruct brain injury incidents to humans [5,15,26,33,36]. While not necessarily an improvement over the use of animal or cadaver impacts in investigations into the mechanism of brain injury, these methods allow for a more accessible method to reconstruct TBI or concussion both financially and for available subjects and/or ethics. The most common computational models for brain injury research as multibody dynamic models and finite element models, but they are used primarily for different roles. Multibody dynamic models are used to simulate the event which led to the brain injury, using the body positions described by witnesses/video or the subject [1,23]. This allows for a simulation to be created which attempts to reproduce the nature of the impact

parameters such as inbound velocity, mass, location, and contact characteristics of the object impacted. The output of this impact simulation is represented in three dimensional loading curves which represent the kinematics of the head [27]. These loading curves can then be used as input for more complex finite element models which are approximate representations of the geometry and material of the human brain [6,27,36]. This allows for the examination of brain deformation in regions of interest which have been proposed to have better links to brain injury than kinematics alone [5,14]. A second common method to generate the loading curves for finite element simulations of the human brain is to use physical headforms to reconstruct the impact. This method is similar to the multibody simulations in that it attempts to reconstruct the impact parameters to generate the input for an FE simulation. However, instead of simulating the environment the researchers would obtain the necessary parameters (mass, velocity, impacted material etc) and then impact the headform in the same place as the subject. The resulting output is then used for the FE simulation. In the literature there are examples of the use of both methods in terms of examinations of brain injury mechanisms and thresholds. However, unlike cadaver and animal model based research, the difference in FE response produced by these two methodologies for brain injury reconstruction has not been elucidated. A better understanding of the influence of these two approaches on the FE outcome would be useful when comparing research using the two methodologies to investigate brain injury, especially when it comes to placing context about the results of this research in terms of the current literature on traumatic brain injury and concussion. As a result, the purpose of this research was to examine the effect of these two different reconstruction methods on the FE simulations of the human brain for the purposes of TBI and concussion research.

Methodology

Experimental Testing

For this research, real life falls with a resulting TBI lesion was selected for reconstruction from Ireland's National Department of Neurosurgery at Beaumont Hospital, Dublin. Each patient signed informed consent forms and all procedures were approved by ethics boards. Simple falls without complicating motions (such as contact with other people) were chosen to reduce the possible number of iterations in the modeling process. Each case had a computed tomography (CT) scan and clinical assessments were conducted by a radiologist and medical doctor at the hospital. The site in which the fall occurred was examined to establish the parameters of the reconstructive environment as well as the height of the fall, and the type of impact surface. In each of the cases the impact occurred against rigid planar surfaces such as concrete or steel. In total six cases were found which met these criteria and were reconstructed using both Mathematical Dynamic Models (1999), (MADYMO™) multibody dynamics software as well as Hybrid III 50% anthropometric dummy headform attached to a monorail drop rig by a Hybrid III neckform.

Brain injury reconstructions for pedestrian accidents and simple falls are commonly conducted using MADYMO because it has a wide variety of human models to choose from [1]. For the fall reconstructions in this research, ellipsoid pedestrian models were chosen which best matched the anthropometry of the real human subjects in these cases. These pedestrian models have been validated against full body pedestrian impacts, however the head contact characteristics were altered to be closer to real skull responses based upon Yoganandan et al's [34] head response curves from tests to cadaver skulls. For each case, a pedestrian model which best represented the individual that was injured was placed within the accident environment. To accomplish the

reconstruction, initial conditions were applied to the simulation based upon accident reports and eyewitness accounts. As it was impossible to be certain what the initial conditions were which caused the fall, a sensitivity analysis was conducted which took the original simulation conditions (X, Y, and Z components in linear and angular velocity, and initial joint rotations/positions) and conducted a reconstruction with no changes, and with these parameters at +/- 10 and 50 %. The resulting linear and rotational accelerations were then applied to the University College Dublin Brain Trauma Model (UCDBTM) to determine the brain deformation incurred at each TBI region of interest (ROI) as defined in the CT scan. The velocity of the head at impact was used as the target velocity for the Hybrid III reconstructions of the same incidents.

The falling reconstructions with the Hybrid III headform were conducted using a monorail drop rig. The Hybrid III 50% headform and neckform was attached to the rail by ball bushings and carriage to reduce the effects of friction (Figure 1). The attachment at the base of the neckform allowed for movement of the head upon impact in 6 degrees of freedom. The impact velocity which was determined from the MADYMO simulations was measured within 0.02 m of the impact anvil by photoelectric time gate. In total, three impacts per simulation were conducted. In the case of this research, the lowest measured head impact velocity derived from the sensitivity analysis was utilized as this was considered to be the lowest possible velocity which caused the resulting lesion (Table 1). The anvil at the base of the monorail was changed to match the impact surface as described in the accident reports used for the MADYMO simulations (Table 1). As with the MADYMO simulations, the impact location on the headform was determined from accident reports. The Hybrid III 50% headform was equipped with a 3-2-2-2 accelerometer array [24] for the measurement linear and rotational acceleration of the headform motion in three dimensions. The accelerometers were Endevco

(Capistrano, CA) 7264C-2KTZ-2-300. The data collection was sampled at 20 kHz with a 1650 Hz lowpass Butterworth filter using DTS TDAS Pro lab module software. The resulting three dimensional acceleration loading curves were applied to the UCDBTM with the same ROI as those identified for the MADYMO simulations from the CT scans (Figure 2).

Computational Modeling

The finite element model used for this research is a modified version of the UCDBTM which was developed by Horgan and Gilchrist [12,13] which was comprised of the following parts: dura, cerebrospinal fluid (CSF), pia, falx, tentorium, grey and white matter, cerebellum, and brain stem (Table 2). The geometry of the head and brain was developed from a male cadaver. The UCDBTM was validated against intracranial pressure responses from Nahum et al's [21] cadaver impacts as well as brain motion from Hardy et al's [10] research. Further validations were undertaken by reconstructing real world TBI injuries and the model was found to be in good agreement with the lesions in comparison with the CT scans [5,26].

The material characteristics (Table 2 and 3) of the UCDBTM were derived from the literature [35]. A linearly viscoelastic material model combined with large deformation theory was used to model the brain [12,13,30,37]. The compressive nature of the brain was considered elastic, and the shear characteristics of the brain were:

$$G(t) = G_\infty + (G_0 - G_\infty)e^{-\beta t}$$

where G_∞ is the long term shear modulus, G_0 is the short term shear modulus and β is the decay factor [12]. A hyperelastic material model was used for the brain in shear in conjunction with a viscoelastic material property. The hyperelastic law was given by:

$$C_{10}(t) = 0.9C_{01}(t) = 620.5 + 1930e^{-t/0.008} + 1103e^{-t/0.15} \ (Pa)$$

where C_{10} and C_{01} are the temperature-dependent material parameters, and t is time in seconds. The compressive behaviour of the brain was considered elastic. The skull brain interaction was modeled by using solid elements to model the CSF with a high bulk modulus and a low shear modulus. As it is currently not possible to simulate a fully coupled fluid dynamics and structural analysis in ABAQUS use was made of the hybrid elements available in this software [12]. Near-incompressible behaviour occurs when the bulk modulus is much larger than the shear modulus (poisson's ration in excess of 0.48) and exhibits behaviour approaching the incompressible limit: where very small changes in displacement results in extremely large changes in pressure [12]. Therefore, a displacement based solution was too sensitive to be used numerically. This singular behaviour was removed from the calculations in ABAQUS by treating the pressure stress as an independently interpolated basic solution variable, coupled to the displacement solution through the constitutive theory and the compatibility condition [12,13]. This independent interpolation of pressure stress is the basis of the hybrid element in this case. The contact definitions in the skull and brain region allowed for no separation and used a friction coefficient of 0.2 [19].

The brain deformation measures used were: pressure, maximum principal strain (MPS), von Mises stress (VMS), shear stress, shear strain, strain rate, and product of strain and strain rate. An analysis was also conducted to determine if the ROI for the TBI lesion was different from the rest of the cerebrum by averaging the values for each element in the ROI and comparing against the cerebrum by means of a t-test.

Brief Case Study Description

Case 1

The first case involved a 76 year old lady who fell backwards while standing on a step. She fell backwards, hitting her head on a vertical concrete wall. Examination of the patient indicated that she incurred an impact to the occipital bone, and CT scans indicated a parenchymal hemorrhage in the right temporal lobe, and a subarachnoid hemorrhage on the left frontal lobe.

Case 2

The second case involved an 85 year old man who lost his balance and hit his forehead on the ground. The impact surface was determined to be the concrete footpath he was walking on. Examination of the patient indicated that the impact was frontal, high up on the head. The CT scans of the patient identified a right acute subdural hematoma.

Case 3

The third case involved an 84 year old woman who also lost her balance on a concrete path. She fell to her right and landed hitting her head in the right frontal area as identified by scratches and bruises. The CT scan identified a left sided subdural hematoma which resulted in a midline shift.

Case 4

The fourth case involved an 85 year old woman who tripped on a concrete footpath. As a result she fell forwards and to the right, hitting the right side of her face and head on the concrete. Examination of the CT scans identified a right side acute subdural hematoma.

Case 5

The fifth case involved a 76 year old gentleman who tripped on a protruding gate stop and fell forwards, slightly to the left of centre. Upon examination, it was identified that the right side of the chin as there were no obvious signs of trauma to any other part of the head. The contact surface was concrete. The ensuing CT scan identified a left side subdural hematoma.

Case 6

The sixth case involved an 87 year old woman who slipped outside her house. The ensuing fall led to an impact to the front right side of her head on a steel railing on the side of the path. It was reported that after hitting her head on the metal beam there was no secondary head contact with the ground or any other object. Upon examination, it was identified that the right frontal area of the skull was the point of contact, and the CT scan indicated a left side subdural hematoma.

Results

The results comparing the MADYMO and Hybrid III dynamic response are presented in Table 4. Sample resultant linear and rotational acceleration loading curves for the MADYMO reconstructions and Hybrid III reconstructions can be found in Figures 3 and 4. The results comparing the MADYMO and Hybrid III based UCDBTM simulations are presented in Tables 5 and 6. The version of the UCDBTM used was not adjusted to represent the brain atrophy that would likely be present for elderly patients. Of the six cases analyzed there were seven discrete regions of interest for analysis by the UCDBTM. The peak mean dynamic response indicated that the peak resultant mean linear acceleration responses were of a larger magnitude when the Hybrid III headform was used in all cases except for case 5, which were roughly equivalent. For peak

resultant mean rotational acceleration the Hybrid III headform reconstruction produced larger magnitudes in all cases except for cases 1 and 6. The peak mean MPS and shear strain values were larger for the Hybrid III reconstructions for cases 1, 3, 4, and 5, and equivalent for case 2. Only case 6 had MADYMO results which produced higher peak mean values in MPS and shear strain. The peak mean strain rate was consistently lower for the MADYMO simulation, and peak mean product of strain and strain rate was larger for the Hybrid III reconstruction in two of the seven regions of interest. The peak mean pressure, VMS, and shear stress were higher for the Hybrid III reconstruction for cases 1 to 5, with the only exception in case 2 being for the subdural hematoma VMS which was lower. Case 6 peak mean pressure response was larger for the Hybrid III reconstruction, but the peak mean VMS and shear stress were lower. Overall, the peak mean strain based and pressure, VMS, and shear stress responses were larger when the Hybrid III headform was used for the reconstruction when compared to using a MADYMO simulation. When comparing the peak mean ROI values to the peak cerebellar values, all the ROI magnitudes were found to be significantly different ($p<0.05$).

Discussion

The purpose of this research was to examine how the use of different reconstruction models influence the results of the UCDBTM simulation for brain injury analysis. The MADYMO method of injury reconstruction is a full body system, where the fall is simulated kinematically and the response of the head impacting the ground was used as input for the UCDBTM. The Hybrid III headform and neckform reconstruction simulated just the head and neck motion upon contact with the ground. As a result, as the inbound velocities and impact locations were matched, the differences in response

between these methods would primarily be found in the contact characteristics of the impact. Of the six cases analyzed, there were seven discrete regions of interest which represented TBI lesions (5 subdural hematoma, 1 contusion, 1 parenchymal hemmorhage). Of those, only case 2 had some results (MPS, VMS, shear strain and shear stress) which were similar regardless of which reconstruction method was used. However, overall the results indicated that the Hybrid III headform provided responses which were of considerably higher magnitude than the MADYMO simulation for all metrics analyzed (pressure, maximum principal strain, von Mises stress, and shear stress and strain). The higher magnitude responses are likely a consequence of the more rigid nature of the Hybrid III in comparison to the deformable model used to simulate the skull in MADYMO simulations. The strain rate was consistently lower for the Hybrid III reconstructions, but those differences may be found in how the metric was calculated, whereas in this case an average value was derived from time to peak of the MPS, the MADYMO FE output may have been an instantaneous value [4,5]. The differences in dynamic response between the MADYMO and Hybrid III reconstructions were not always replicated by the FE results. For example, in case 2 the rotational acceleration response was much larger for the Hybrid III simulations, however the strain results were similar to those from the MADYMO reconstructions. These results indicate that the magnitude of the strains in the regions of interest as was the method of analysis in this research may not be as highly influenced by peak resultant rotational acceleration as the general cerebral responses as has been shown by previous researchers [6,28]. This discrepancy also demonstrates the increased sensitivity of using finite element modeling of the brain in conjunction with medical imaging when it comes to injury prediction over just using the kinematic responses. This difference between regions is also demonstrated by the significant differences between the peak ROI stresses and strains

and the peak cerebellar stresses and strains. These findings reinforce the benefits of examining the output of TBI reconstructions using FE modeling in conjunction with medical scanning to determine the regions of interest of the brain which incurred the damage.

Interestingly, when the results are compared to the literature, the Hybrid III results match well with concussion and TBI research, while the MADYMO simulations produce what would be considered very low local brain deformation responses for TBI lesions. In three of the cases the ROI for subdural hematoma in the MADYMO reconstructions was 0.14 – 0.19 MPS, where Hybrid III response would give 0.274 - 0.481. The MADYMO values would be considered in the concussive range [15,36] whereas the physical model result would be in the TBI range which is consistent with the nature of the injuries in this research [2,16,20]. It is likely that since a great deal of the current concussion data was collected using Hybrid III models the magnitudes of brain deformation and dynamic response may be higher than those from simulations using deformable conditions for the head. This premise is reinforced by anatomical testing indicating that functional injury to tissue can happen as low as 0.1 strain, indicating that its possible that current data using the Hybrid III for concussion threshold research may be artificially high [2,17]. These differences created by the models create biases in the data which must be recognized for the correct interpretation of brain injury data as the tools in use can influence the magnitudes and relationships of results. As a result these considerations must be taken into account when comparing thresholds of brain injury from across the scientific literature.

This work examined the differences using MADYMO and Hybrid III headform for injury reconstruction. This work was conducted because MADYMO full body simulations and monorail impacts using a Hybrid III head and neckform are becoming

common methods to conduct brain injury research and their differences in response need to be identified. As a result this research has certain limitations surrounding the use of these methodologies. The MADYMO software is intended for use in car crash scenarios and not for falling impacts. The authors attempted to account for this fact by using Yoganandan et al's [34] head deformation characteristics for the simulation procedure. Even so, some of the kinematics of the events may not have been identical to those of the actual impact event. The MADYMO reconstructions were estimates of the human response resulting from a fall. Also, the acceleration loading curves generated from the impact in the simulated environment are based upon contact definitions and other assumptions which may not be biofidelic. The Hybrid III headform may be reliable but is limited in its biofidelity. The Hybrid III neackform that was used to attach the headform to the monorail allows for movement in six degrees of freedom, however the nature of that motion if likely stiffer than that of the real human neck and would affect impact responses. The use of a monorail in conjunction with a Hybrid III headform has been used in brain injury research and has produced magnitudes of dynamic response and brain deformation consistent with anatomic research [26]. While not a validation of this injury reconstruction method, it has therefore been shown to produce results that are reasonable in comparison with the literature. As a result, both systems may not produce acceleration loading curves which would represent the true nature of the injuries described in the reports. The finite element model is also a representation of human brain tissue, and as such may not produce the actual brain responses for each injury reconstruction.

Conclusions

In conclusion, when conducting brain injury reconstruction research it is important to account for the type of model used and recognize how it influences the results. In

particular, when comparing brain injury simulations using MADYMO vs Hybrid III headforms to generate dynamic response, the Hybrid III tends to produce much higher magnitudes in acceleration and FE outputs. Additionally, these differences help place previous literature for brain injury reconstruction into context as reconstructions using MADYMO will tend to produce lower values than those reconstructed with a Hybrid III headform. Finally, this work has shown that large magnitude dynamic response may not produce large deformations in the regions of interest of the FE model as identified by CT scans. This result in particular shows the importance of using FE models of the brain to examine the tissue deformation in the regions that were injured as opposed to global linear and rotational acceleration responses. Finally, the authors maintain that each of these tools for brain injury reconstruction in this research has its benefits and drawbacks and neither is inherently better than the other for this purpose.

References

[1] J. Adamec, K. Jelen, P. Kubovy, F. Lopot, and E. Schuller, *Forensic biomechanical analysis of falls from height using numerical human body models*. J. Forensic Sci. 55(6) 2010, pp. 1615-1623.

[2] A.C. Bain and D.F. Meaney, *Tissue-level thresholds for axonal damage in an experimental model of central nervous system white matter injury*. J. Biomech. Eng. 16 2000, pp. 615-622.

[3] D.R. Bradshaw, J. Ivarsson, C.L. Morfey, and D.C. Viano, *Simulation of acute subdural hematoma and diffuse axonal injury in coronal head impact*. J. Biomech. 34 (1) 2001, pp. 85-94.

[4] M.C. Doorly, *Investigations into head injury criteria using numerical reconstruction of real life accident cases*, Ph.D. diss., University College Dublin, 2007.

[5] M.C. Doorly and M.D. Gilchrist, *The use of accident reconstruction for the analysis of traumatic brain injury due to head impacts arising from falls*. Comput. Methods Biomech. Biomed. Eng. 9(6) 2006, pp. 371-377.

[6] M.A. Forero Rueda, L. Cui, and M.D. Gilchrist, *Finite element modeling of equestrian helmet impacts exposes the need to address rotational kinematics in*

future helmet designs. Comput. Methods Biomech. Biomed. Eng. 14(12) 2011, pp. 1021-1031.

[7] E.S. Gurdjian and E.S. Gurdjian ES, *Acute head injury: A review*. Surg. Ann. 12 1980, pp. 223-241.

[8] E.S. Gurdjian and H.R. Lissner, *Mechanisms of head injury as studied by the cathode ray occiloscope: Preliminary report*. J. Neurol. Neurosurg. Psy. 1 1944, pp. 393-399.

[9] T.A. Gennarelli, L.E. Thibault, J.H. Adams, D.I. Graham, C.J. Thompson, R.P. Marcincin, *Diffuse axonal injury and traumatic coma in the primate*. Ann. Neurol. 12 1983, pp. 564-574.

[10] W.N. Hardy, C.D. Foster, M.J. Mason, K.H. Yang, A.I. King, and S. Tashman, *Investigation of head injury mechanisms using neutral density technology and high-speed biplanar x-ray*. Stapp Car Crash J. 45 2001, pp. 337-368.

[11] A.H.S.Holbourn, *Mechanics of head injuries.* The Lancet 242(6267) 1944, pp. 438-441.

[12] T.J. Horgan and M.D. Gilchrist, *The creation of three-dimensional finite element models for simulating head impact biomechanics*. IJCrash 8(4) 2003, pp. 353-366.

[13] T.J. Horgan and M.D. Gilchrist, *Influence of FE model variability in predicting brain motion and intracranial pressure changes in head impact simulations*. IJCrash 9(4) 2004, pp. 401-418.

[14] A.I. King, K. Yang, L. Zhang, and W. Hardy, *Is head injury caused by linear or angular acceleration?* In Bertil Aldman award lecture, Proceedings of the IRCOBI Conference on the Biomechanics of Impact, 2003, pp. 1-12.

[15] S. Kleiven, *Predictors for traumatic brain injuries evaluated through accident reconstruction*. Stapp Car Crash J. 51 2007, pp. 81-114.

[16] M.C. Lee and R.C. Haut, *Insensitivity of tensile failure properties of human bridging veins to strain rate: implications in biomechanics of subdural hematoma*. J. Biomech. 22(6-7) 1989, pp. 537-542.

[17] S.S. Margulies and L.E. Thibault, *A proposed tolerance criterion for diffuse axonal injury in man.* J. Biomech. 25(8) 1992, 917-923.

[18] A.C. McKee, B.E. Gavett, R.A. Stern, C.J. Nowinski, R.C. Cantu, N.W. Kowall, D.P. Perl, E.T. Hedley-White, B. Price, C. Sullivan, P. Morin, H.S. Lee, C.A. Kubilus, D.H. Daneshvar, M. Wulff, and A.E. Budson, *TDPE-43 proteinopathy and motor neuron disease in chronic traumatic encephalopathy.* J. Neuropathol. Exp. Neurol. 69(9) 2010, pp. 918-929.

[19] R. Miller, S. Margulies, M. Leoni, M. Nonaka, Z. Chen, D. Smith, and D. Meaney, *Finite element modeling approaches for predicting injury in an experimental model of severe diffuse axonal injury*. In proceedings of the 42nd Stapp Car Crash Conference, SAE paper No. 983154, 1998.

[20] K.L. Monson, W. Goldsmith, N.M. Barbaro, and G.T. Manle, *Axial mechanical properties of fresh human cerebral blood vessels*. J. Biomed. Eng. 125(2) 2003, pp. 288-294.

[21] A.M. Nahum, R. Smith, C.C. Ward, *Intracranial pressure dynamics during head impact.* In proceedings 21st Stapp Car Crash Conference. SAE paper No. 770922, 1977.

[22] B.I. Omalu, S.T. DeKosky, R.L. Minster, M.I. Kamboh, R.L. Hamilton, and C.H. Wecht, *Chronic traumatic encephalopathy in a national football league player*. Neurosurg. 57 2005, pp. 128-134.

[23] K. O'Riordain, P.M. Thomas, J.P. Phillips, and M.D. Gilchrist. *Reconstruction of real world head injury accidents resulting from falls using multibody dynamics*. Clin. Biomech. 18 2003, pp. 590-600.

[24] A.J. Padgaonkar, K.W. Kreiger, and A.I. King, *Measurement of angular acceleration of a rigid body using linear accelerometers*. J. Appl. Mech. 42 1975, pp. 552-556.

[25] A.Post and T.B. Hoshizaki, *Mechanisms of brain impact injuries and their prediction: A review*. Trauma 14(4) 2012, pp. 327-349.

[26] A.Post, T.B. Hoshizaki, M.D. Gilchrist, and S. Brien, *Analysis of the influence of independent variables used for reconstruction of a traumatic brain injury event*. J. Sports Eng. Tech. 226(3-4) 2012a, pp. 290-298.

[27] A.Post, T.B. Hoshizaki, and M.D. Gilchrist, *Finite element analysis of the effect of loading curve shape on brain injury predictors.* J. Biomech 45 2012b, pp. 679-683.

[28] A.Post, A. Oeur, T.B. Hoshizaki, and M.D. Gilchrist, *The influence of centric and non-centric impacts to American football helmets on the correlation between commonly used metrics in brain injury research*. In Proceedings of the IRCOBI, Dublin, 2012c

[29] S. Shively, A.I. Scher, D.P. Perl, and R. Diaz-Arrastia, *Dementia resulting from traumatic brain injury: What is the pathology?* Arch. Neurol. 69(10) 2012, pp. 1245-1251.

[30] L.Z. Shuck and S.H. Advani, *Rheological response of human brain tissue in shear*. J. Basic. Eng. 94(4) 1972, pp. 905-912.

[31] D.M. Sosin, J.E. Sniezek, and D.J. Thurman, *Incidence of Mild and Moderate Brain Injury in the United States, 1991*. Brain Inj. 10(1) 1996, pp. 47-54.

[32] L.M. Thomas, V.L. Roberts, and E.S. Gurdjian, *Impact-induced pressure gradients along three orthogonal axes in the human skull*. J. Neurosurg. 26(3) 1967, pp. 316-321.

[33] R. Willinger and D. Baumgartner, *Human head tolerance limits to specific injury mechanisms.* IJCrash, 8(6) 2003, pp. 605-617.

[34] N. Yoganandan, F.A. Pintar, Jr. A. Sances, P.R. Walsh, C.L. Ewing, D.J. Thomas, R.G. Snyder, *Biomechanics of skull fractures*. J. Neurotrauma 12(4) 1995, pp. 659-668.

[35] L. Zhang, K. Yang, R. Dwarampudi, K. Omori, T. Li, K. Chang, W.N. Hardy, T.B. Khalil, and A.I. King, *Recent advances in brain injury research: A new human head model development and validation*. Stapp Car Crash J. 45 2001, pp. 369-393.

[36] L. Zhang, K.H. Yang, and A.I. King, *A proposed injury threshold for mild traumatic brain injury*. J. Biomech. Eng. 126 2004, pp. 226-236.

[37] A.Zhou, T.B. Khalil, A.I. King, *A new model for comparing responses of the homogeneous and inhomogeneous human brain*. In proceedings of the 39th Stapp Car Crash Conference, 1995, pp. 121-136.

Table 1. Impact surfaces and inbound velocities for the fall reconstructions

Case #	Impact Surface	Velocity (m/s)
1	Concrete	4.8
2	Concrete	5.1
3	Concrete	4.5
4	Concrete	3.5
5	Concrete	4.7
6	Steel	5.4

Table 2. Material characteristics of the brain for the UCDBTM

Material	Poisson's Ratio	Density (kg/m^3)	Young's Modulus (Mpa)
Dura	0.45	1130	31.5
Pia	0.45	1130	11.5
Falx	0.45	1140	31.5
Tentorium	0.45	1140	31.5
CSF	0.5	1000	-
Grey Matter	0.49	1060	Hyperelastic
White Matter	0.49	1060	Hyperelastic

Table 3. Material characteristics of the brain for the UCDBTM

Material	Shear Modulus (kPa)		Decay Constant (s^{-1})	Bulk Modulus (GPa)
	G_0	G_∞		
White Matter	12.5	2.5	80	2.19
Grey Matter	10	2	80	2.19
Brain Stem	22.5	4.5	80	2.19
Cerebellum	10	2	80	2.19

Table 4. Comparison of the dynamic response of the MADYMO simulation and the Hybrid III impacts. Standard deviation in brackets.

			Acceleration	
Case #	Model	Velocity (m/s)	Linear (g)	Rotational (krad/s^2)
1	MADYMO	4.8	236.5	33.88
	Hybrid III	4.8	448.0 (15.1)	31.67 (0.7)
2	MADYMO	5.1	340.8	15.21
	Hybrid III	5.1	686.9 (50.5)	54.93 (2.7)
3	MADYMO	4.5	354.8	27.84
	Hybrid III	4.5	529.6 (32.3)	37.84 (1.7)
4	MADYMO	3.5	243.2	16.06
	Hybrid III	3.5	327.8 (14.1)	36.32 (1.7)

5	MADYMO	4.7	305.6	11.54	
	Hybrid III	4.7	274.4 (12.4)	55.52 (2.9)	
6	MADYMO	5.4	329.4	45.19	
	Hybrid III	5.4	366.3 (17.2)	31.61 (2.8)	

Table 5. Model comparisons for the strain based results from the UCDBTM simulations. Standard deviation in brackets.

Case #	Lesion	Model	MPS	Shear strain	Strain rate (s^{-1})	Product of strain and strain rate (s^{-1})
1	Parenchymal Hemorrhage	MADYMO	0.16	0.26	132	14.7
		Hybrid III	0.304 (0.007)	0.462 (0.006)	40.2 (4.6)	12.2 (1.4)
1	Contusion	MADYMO	0.18	0.25	145	20.1
		Hybrid III	0.279 (0.012)	0.506 (0.024)	39.0 (2.4)	10.9 (1.1)

Case #	Lesion	Model	Pressure (kPa)	VMS (kPa)	Shear stress (kPa)
2	Subdural Hematoma	MADYMO	0.29	0.45	190	23.9
		Hybrid III	0.288 (0.012)	0.441 (0.019)	44.5 (16.3)	12.7 (4.2)
3	Subdural Hematoma	MADYMO	0.19	0.26	147	19
		Hybrid III	0.391 (0.013)	0.544 (0.017)	62.5 (1.8)	24.5 (1.5)
4	Subdural Hematoma	MADYMO	0.14	0.17	166	16.6
		Hybrid III	0.481 (0.017)	0.483 (0.01)	137.5 (6.7)	66.2 (5.5)
5	Subdural Hematoma	MADYMO	0.15	0.26	151	15.0
		Hybrid III	0.303 (0.015)	0.592 (0.027)	39.6 (2.0)	12.0 (1.2)
6	Subdural Hematoma	MADYMO	0.53	0.5	348	140
		Hybrid III	0.347 (0.018)	0.452 (0.034)	44.7 (2.9)	15.5 (1.8)

Table 6. Model comparisons for the pressure, von Mises stress and shear stress results from the UCDBTM simulations. Standard deviation in brackets.

1	Parenchymal	MADYMO	58.59	5.53	2.55
	Hemorrhage	Hybrid III	767.5 (18.2)	9.88 (0.18)	4.50 (0.05)
1	Contusion	MADYMO	111.8	5.82	2.22
		Hybrid III	1063.1 (24.5)	10.1 (0.14)	4.77 (0.18)
2	Subdural	MADYMO	308.5	9.98	4.53
	Hematoma	Hybrid III	1218.0 (120)	9.10 (0.31)	4.11 (0.13)
3	Subdural	MADYMO	171.3	7.11	2.53
	Hematoma	Hybrid III	921.6 (19.8)	12.2 (0.41)	5.03 (0.17)
4	Subdural	MADYMO	227.9	5.23	1.80
	Hematoma	Hybrid III	651.5 (11.4)	15.6 (0.57)	4.62 (0.99)
5	Subdural	MADYMO	149.5	5.17	2.45
	Hematoma	Hybrid III	847.0 (103)	11.8 (0.11)	5.04 (0.09)
6	Subdural	MADYMO	55.6	17.0	4.75
	Hematoma	Hybrid III	718.9 (66.4)	9.95 (0.62)	4.21 (0.15)

Figures

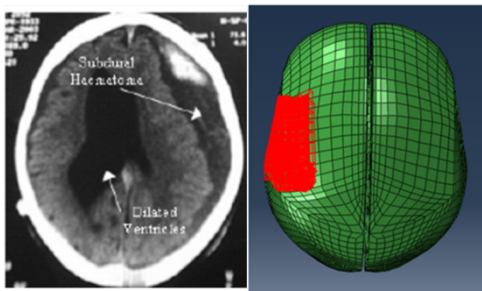Figure 1. Hybrid III reconstruction of a fall.

Figure 2. Example of Case #3's regions of interest representing the subdural hematoma in the UCDBTM. On the CT, the left side of the image is the right side of the brain and vice versa.
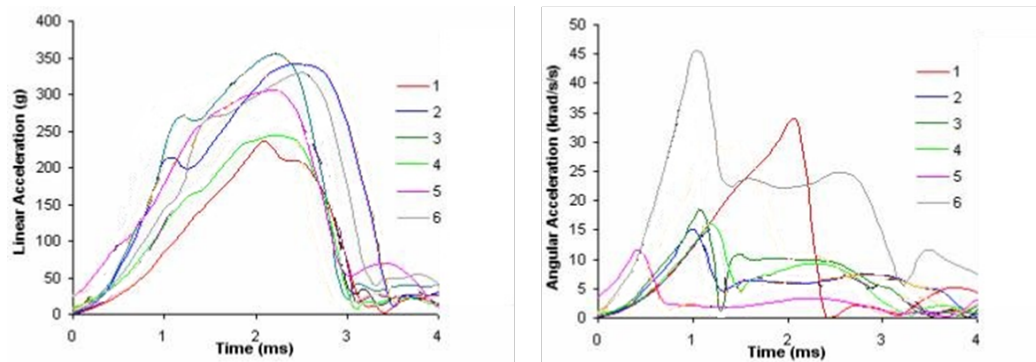

Figure 3. Sample peak resultant linear (left) and rotational (right) acceleration loading curves for cases 1 – 6 for the MADYMO reconstructions.
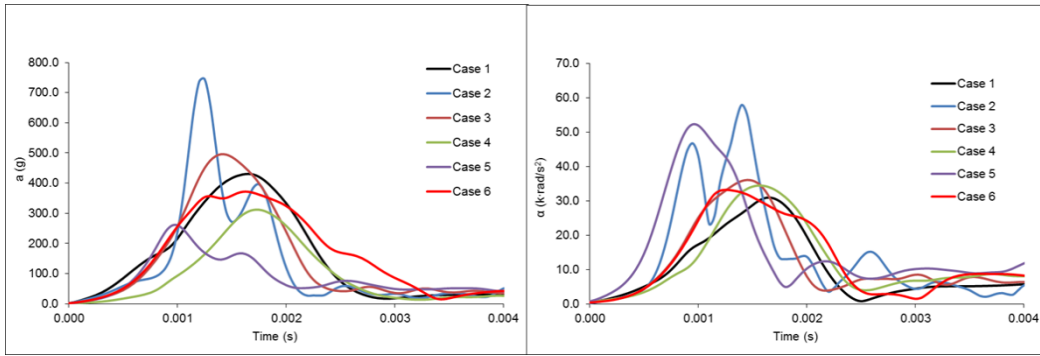
Figure 4. Sample peak resultant linear (left) and rotational (right) acceleration loading curves for cases 1 – 6 for the Hybrid III reconstructions.